Atomic processes in molecular beam epitaxy on strained InAs(137): A density-functional theory study

P. Kratzer[1,2,*] and T. Hammerschmidt[2,3]

[1]*Fakultät für Physik, and Center for Nanointegration (CeNIDE), Universität Duisburg-Essen, Lotharstrasse 1, D-47048 Duisburg, Germany*

[2]*Fritz-Haber-Institut der MPG, Faradayweg 4-6, D-14195 Berlin, Germany*

[3]*Interdisciplinary Centre for Advanced Materials Simulation (ICAMS), Ruhr-Universität Bochum, Stiepeler Strasse 129, D-44801 Bochum, Germany*

(Received 28 April 2009; revised manuscript received 3 July 2009; published 28 July 2009)

The atomic processes in molecular beam epitaxy of InAs on the InAs(137) surface are investigated by means of first-principles total-energy calculations. We consider layer-by-layer growth on InAs(137) facets as a typical process during the evolution of shallow InAs islands in the Stranski-Krastanov growth mode of InAs on GaAs that is exploited for the self-assembly of heteroepitaxial quantum dots. From the calculated energetics we conclude that a growth scenario where an As_2 molecule adsorbs on a single In adatom, followed by capture of another In adatom, is most likely. Moreover, our calculations of the potential-energy surface for In adatoms on the InAs(137) surface show that In adatoms are highly mobile. Surface diffusion on InAs(137) is found to be almost isotropic with energy barriers <0.3 eV for adatom hopping. Aiming at an understanding of the growth processes at the strained side facets of quantum dots, we extend our calculations to isotropically strained InAs(137) facets. It is found that the compressive strain present on side facets of shallow InAs islands on GaAs leads to a considerable lowering of the binding energy of In adatoms. The height of diffusion barriers is found to be less affected by the strain. Most importantly, the intermediate species consisting of an In adatom plus an adsorbed As_2 molecule is destabilized by compressive strain in excess of -5%. This finding leads us to the conclusion that layer growth on InAs(137) facets ceases in highly strained regions of InAs islands on GaAs, in line with the observed shape evolution of such islands.

DOI: 10.1103/PhysRevB.80.035324 PACS number(s): 68.43.Jk, 68.55.A−, 81.05.Ea, 68.65.Hb

I. INTRODUCTION

The discovery of stable high-index surface orientations of the *III-V* semiconductors, in particular GaAs and InAs (for a review, see Ref. 1), has opened up exciting prospects for epitaxial growth. The stable surfaces of (113) or (2 5 11) orientation can be used both for growing smooth films in homoepitaxy as well as for fabricating self-assembled quantum dots (QDs) in heteroepitaxy of InAs on GaAs.[2–4] So far, the atomistic processes during growth on high-index surfaces of *III-V* semiconductors have received little attention. In this paper, we present a theoretical study of elementary processes of growth on InAs(137), a structurally simple high-index surface.

To provide a unified picture of the high-index *III-V* surfaces, we emphasize that their atomic structure consists of similar structural motifs as found on the (001) and (111) surfaces of these materials: These are threefold coordinated As atom, threefold coordinated Ga or In atoms, as well as As dimers or cation dimers, on the *A*- or *B*-type orientations, respectively. In the following, we will concentrate on the *A*-type surfaces, which display As dimers as structural motifs. Compared to the (001) surface, where such dimers lie within the surface plane, the As dimers are arranged in "staircase patterns" on the high-index surfaces (see Fig. 1). The As-As bond, pointing along the $(1\bar{1}0)$ direction, is slightly inclined with respect to the surface plane. One As dimer, two threefold coordinated cations, and one threefold coordinated As atom form the smallest structural unit of these surfaces (one "step" in the staircase). Periodic repetition of these units results in a surface with (137)*A* orientation. At the stable (2 5 11)*A* surfaces, three such structural units plus one threefold coordinated cation fill up the unit mesh.[5–7] The other stable high-index surface, the (113)*A* orientation, results from a very complex arrangement of the same structural units, the so-called (8×1) reconstruction.[8,9]

Here, we employ density-functional theory (DFT) calculations to investigate the elementary growth processes on InAs(137)A. Since this surface contains already all structural motifs of the more complex (2 5 11)*A* and (113)*A*(8×1) surfaces, it may serve as an example to study adsorption, surface diffusion, and nucleation on high-index substrates. Moreover, InAs(137)*A* is relevant since this surface orientation has been found to occur as side facet on InAs quantum dots grown on various GaAs substrates.[10–12] In a recent theoretical study, we suggested that the shape evolution of these

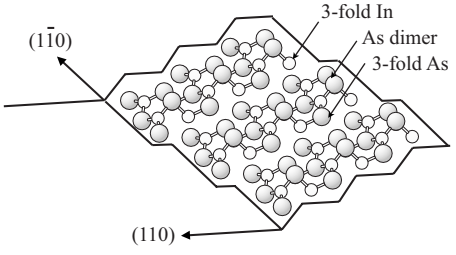

FIG. 1. The InAs(137) surface plane is inclined relative to both the (100) and the $(1\bar{1}0)$ directions. One surface unit cell contains an As dimer, two threefold coordinated cations (one of which is visible in the figure), and one threefold coordinated As atom.

quantum dots is governed by the layer-by-layer growth mode of their (137) side facet.[13] As the side facets of quantum dots are considerably strained, we will investigate how compressive strain affects the energetics of the various elementary processes of epitaxial growth on InAs(137)*A*.

II. METHOD OF CALCULATION

We performed total-energy DFT calculations using the computer program FHI98MD (Ref. 14) to determine the adiabatic potential-energy surface (PES) for surface diffusion of an In adatom. Within the supercell approach, the surface was represented by a 15-Å-thick slab, separated from its periodic image by a vacuum layer of 11 Å. At the bottom surface, In and As dangling bonds are passivated by pseudo-H atoms with an artificial nuclear charge of $Z=1.25$ and $Z=0.75$, respectively. The lateral periodicity of the supercell was (2×2), i.e., in both directions a factor 2 larger than the periodicity of the InAs(137) surface, in order to minimize artificial interactions between periodic images of the adatom. Equilibrium surface geometries are obtained by atomic relaxation until the residual forces $\lesssim 0.025$ eV/Å, keeping the bottom layer and pseudo-H atoms fixed. Brillouin-zone (BZ) integration was carried out using a regular mesh[15] of $2\times2\times1$ points. Test calculations with $2\times4\times1$ mesh showed that adsorption energies are converged to within 0.05 eV with this **k**-point set. Kohn-Sham orbitals were expanded in-plane waves up to a cutoff energy of 10 Ry. The Perdew-Burke-Ernzerhof (PBE) generalized gradient approximation[16] was employed to describe the electronic exchange and correlation interaction. *Ab initio* norm-conserving pseudopotentials are used for all species.[17] These were constructed using the highest *s* and *p* states of Ga, In, and As as valence states. The occupation of the electronic bands has been calculated using a broadening of the Fermi distribution with an artificial electronic temperature corresponding to 0.1 eV, and the thus obtained total energies were extrapolated to zero electronic temperature.

With these settings, the PES is obtained by calculating the binding energy E_b of the In adatom on a discrete grid of 7×10 points $\{X,Y\}$ in the InAs(137) unit cell. As the energy zero we choose the sum of total energies of the slab representing the clean surface and of an isolated spin-polarized In atom. For fixed (X,Y) the Z coordinate of the adatom is optimized starting from a value 2.5 Å higher than the z coordinate of the closest surface atom. All substrate atoms, with the exception of the pseudo-H atoms and the lowest As and In atoms attached to them, are allowed to relax. The final "map" of the PES is obtained by interpolating the calculated points with bicubic splines.

III. RESULTS

A. In adatom diffusion on InAs(137)

While the surface unit cell of the experimentally stable reconstruction of InAs(2 5 11)*A* contains three subunits of As dimers [for the atomic structure, cf. the analogous reconstruction of GaAs(2 5 11)*A* (Refs. 5 and 6)], the surface unit cell of InAs(137) consists of only one such subunit. Consequently, the (137)*A* surface does not obey the electron counting rule but is formally deficient of 1/4 of elementary charge per unit cell. Hence the (137)*A* surface is intrinsically *p* type and has its Fermi level located near the top of the valence band. Despite its violation of the electron counting rule, the InAs(137) surface has a low surface energy of 39.5 meV/Å^2, very close to the surface energy of the InAs(2 5 11)*A* surface of 38 meV/Å^2. (Both values are quoted for equilibrium with an As-rich environment.) As has been demonstrated by DFT calculations in Ref. 13, the surface energy of InAs(137) is lowered considerably if this surface is subject to compressive strain. Hence the occurrence of (137)*A* as (compressively strained) side facet of InAs quantum dots on GaAs can be understood from the principle of energy minimization.

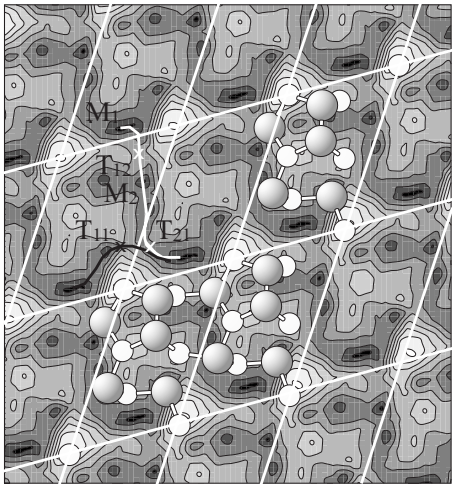

FIG. 2. Potential energy surface for diffusion of an In adatom on InAs(137). The most important minima are labeled M_1 and M_2 (the latter is a double minimum). Energy barriers on the paths connecting these minima are labeled T_{11}, T_{12}, and T_{21}. Two diffusion pathways are indicated, the "uphill" diffusion pathway (black curve) involving T_{11} and the "sideways" diffusion pathway (white curve) involving T_{12}, M_2, and T_{21}.

The potential-energy surface for an In atom on the InAs(137) surface as obtained from our DFT-PBE calculations is displayed in Fig. 2. The exact value of the In adsorption energy depends on the surface site. We find that the In atom is bound by 2.5–2.8 eV. This large binding energy ensures that thermal evaporation of In atoms from this surface is negligible under the typical growth temperatures of 400–500 °C. The most strongly bound site is the hollow site between the threefold coordinated As atom and the As dimer (indicated as M_1 [Fig. 3(a)]). The second-most stable site is located next to the center of the As-As dimer bond in a position where its orbitals overlap with one of the fourfold coordinated surface As atoms below [M_2 in Fig. 3(b)]. Thus, M_2 actually corresponds to two nearby sites that are energetically almost degenerate. In addition, the PES displays several other more shallow minima, which we believe to be less important for growth. We note that a single In adatom acts as an electron donor on InAs(137) and transfers part of its charge to the (not fully occupied) valence band of the slab. For adatom concentrations corresponding to one In atom in

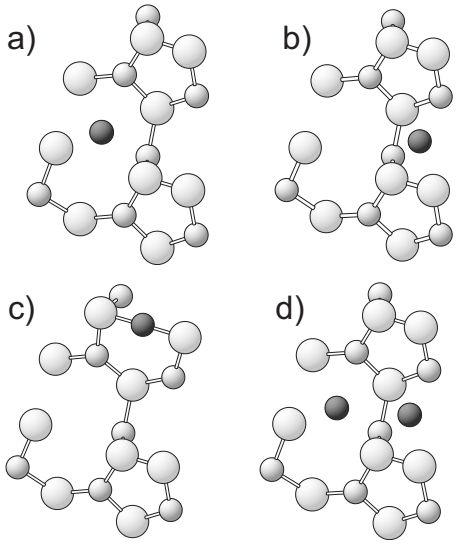

FIG. 3. Atomic geometries after relaxation, as obtained from our DFT calculations, (a) for an In adatom in site M_1, (b) for an In adatom in site M_2, (c) for an In adatom in site M_D inside the As surface dimer, and (d) for two In adatoms occupying both M_1 and M_2.

the 2×2 unit cell chosen in our calculations, the Fermi level is located at the valence-band top, even after In adsorption.

In addition to our calculations of the *on-surface* PES of In/InAs(137)*A*, we investigated a peculiar growth process that is known from the case of Ga/GaAs(001) $\beta2(2\times4)$. There, DFT calculations have shown that Ga adatoms have the ability to break the As-As bond of As surface dimers.[18] Later it was demonstrated that this splitting of surface As dimers by Ga adatoms is one of the key processes in homoepitaxy.[19] Therefore we studied the analogous process of an In adatom on InAs(137)*A* splitting the As surface dimer. Our calculations show that the configuration M_D, with an In atom sitting in the bond axis of a broken As dimer, is a metastable local minimum with an energy of −2.62 eV. However, its energy is higher than the energy of In adatoms at both *on-surface* adsorption sites, by 0.16 eV compared to M_1. Hence we conclude that breaking the surface As dimer bond is *not* the process that initiates epitaxial growth on InAs(137), in contrast to the case of Ga/GaAs(001), where the corresponding M_D is lower than the on-surface binding energies. This finding is in line with previous computational results from our group demonstrating that the broken surface As dimer bond of the GaAs(001) $c(4\times4)$ surface[20] or of the $In_{2/3}Ga_{1/3}As(001)$ (2×3) wetting layer[21] is energetically less favorable for indium than the corresponding on-surface sites. Only on an InAs wetting layer of 1.75 ML thickness on GaAs(001), displaying the $\beta2(2\times4)$ reconstruction, recent calculations[22] find an energetic preference of In to insert into the As dimers in the trench of this reconstruction. These examples show that the In atom, which is more bulky compared to a Ga atom and forms weaker bonds with arsenic, is rarely able to insert itself into surface As dimer bonds.

Next, we discuss indium diffusion on InAs(137)*A*. As can be seen from Fig. 2, there are two dominant diffusion pathways. The first one (black curve in Fig. 2) connects directly

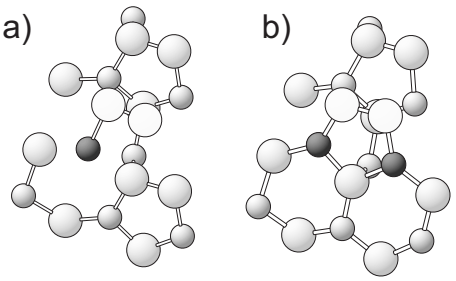

FIG. 4. Atomic geometries after relaxation, as obtained from our DFT calculations, (a) for an As_2 molecule adsorbed on an In adatom in site M_1 and (b) for an As_2 molecule adsorbed on In adatoms in sites M_1 and M_2.

adjacent periodic images of adsorption site M_1 via transition state T_{11}. We refer to this pathway as "uphill" diffusion as it leads to an upward diffusion within the "staircase" picture of the (137)*A* surface, corresponding to an uphill diffusion at the side facet of a QD. Along the second diffusion path (black curve in Fig. 2) the In atom first moves from M_1 to the double minimum M_2 by overcoming the energy barrier at T_{12}, then traverses transition state T_{21} to join the "uphill" diffusion pathway, and reaches a periodic image of M_1. We call this second pathway "sideways" diffusion, again in analogy to diffusion on the (inclined) side facets of a QD. The values of the maximum energy barriers along either pathway (0.26 and 0.29 eV, respectively) are comparable to those calculated earlier for In diffusion on an $In_{2/3}Ga_{1/3}As$ wetting layer on GaAs(001) with (2×3) reconstruction[21] and somewhat lower than the barriers reported for In diffusion on InAs(001) in the $\beta2(2\times4)$ reconstruction[23] and In diffusion on the $\beta2(2\times4)$ reconstructed wetting layer (1.75 ML InAs) on GaAs(001).[22,24] We note that the energy barriers for "uphill" diffusion and "sideways" diffusion are of comparable size, i.e., long-range diffusion on the unstrained InAs(137) surface is nearly isotropic.

B. Intermediate stages of growth

Previous theoretical[25] and experimental studies[26] have found that the chemically rather stable As_2 molecule (and even more so the As_4 molecule) binds only weakly to an As-rich *III-V*-semiconductor surface. Adsorption of the cation species (here: of indium adatoms) is required before As_2 molecules can be adsorbed more strongly. Therefore we restrict ourselves to two growth scenarios: (i) adsorption of an As_2 molecule to a single In adatom in its most favorable adsorption site [Fig. 3(a)], leading to the intermediate structure shown in Fig. 4(a), followed by capture of another diffusing In adatom, and eventually leading to the structure in Fig. 4(b); (ii) formation of a pair of In adatoms in neighboring adsorption sites [Fig. 3(d)], followed by adsorption of As_2 on both these In adatoms, and again leading to the configuration shown in Fig. 4(b).

In order to assess which of the two growth scenarios is more likely, we first investigate the interaction of two In atoms in adjacent adsorption sites. Our DFT calculations show that the configuration with two neighboring In atoms

[Fig. 3(d)] is energetically higher than two individual In atoms at separated M_1 sites. Hence, the interaction between neighboring In atoms is repulsive. To some extent, this can be traced back to the charge state of the In atoms: as mentioned earlier, the In atoms donate one electron to the valence band and thus are positively charged. For two In atoms in the (2×2) unit cell used in our calculations, this charge donation is not fully developed as the Fermi level remains pinned in an In-induced gap state at a coverage of two In atoms. Hence, two adjacent In adatoms cannot lower their energy as much as two infinitely separate In adatoms. In order to assess the effect of the Fermi-level pinning, which may not occur on a real surface with other defects or impurities present, we repeat the calculations with a charged unit cell where one electron has been removed, thus mimicking a strongly *p*-type substrate. Again, also under conditions where both In adatoms donate charge to the valence band, we find that the interaction is repulsive compared to isolated In adatoms under the same conditions. In addition, we performed a calculation for an initial structure with two In atoms forming an As-In-As-In-As zig-zag chain (after the As dimer bond is broken). However, this structure is found to be energetically higher than the one depicted in Fig. 3(d). We thus conclude that a configuration with two In adatoms in neighboring sites is rather unstable and unlikely to form during growth.

Next, we investigate the binding energy of As_2 molecules to the surface in the configurations in Figs. 4(a) and 4(b). In these figures, the adsorbed As_2 is shown as white balls, while surface As is shown in light gray. Note that the surface As dimers are intact in Fig. 4(a), whereas one surface As dimer is broken by an inserted In atom in Fig. 4(b). The adsorption energy, i.e., the energy differences between these structures and the corresponding adatom structures in Fig. 3 plus the energy of a free As_2 molecule in the gas phase, is decisive for the possible role of As_2-In complexes as growth intermediates. Our DFT calculations yield adsorption energies of 0.60 and 1.55 eV for As_2 bound to one In adatom [Fig. 4(a)] and to two In adatoms [Fig. 4(b)], respectively. Considering the reverse process, desorption of As_2, the average lifetime of these structures at a typical growth temperature of 400° may be estimated from the Arrhenius law. Assuming a preexponential factor of 10^{13} sec^{-1}, we obtain an average lifetime of about 3 ns or 0.04 s for the As_2 species bound to one or two In adatoms, respectively. The lifetime of the As_2-In complex is thus very short on an experimental time scale. Yet, its lifetime of 3 ns is more than 350 times longer than the hopping frequency of a free In adatom during surface diffusion on InAs(137)*A*. Hence it is likely that a diffusing In adatom reaches the As_2-In complex before the latter decays via desorption, resulting in formation of the much more long-lived In-As_2-In complex of Fig. 4(b). We conclude that the structure in Fig. 4(a) must be considered as an important intermediate stage during growth. From the two growth scenarios discussed above, scenario (i), growth via an intermediate As_2-In complex, is clearly more likely than scenario (ii) as the concentration of In adatom pairs will be negligibly small due to the repulsive In-In interaction. This means that the breaking of the As surface dimer bond (that is a prerequisite for continuing growth by a new layer of material) takes place between the configurations shown in Figs. 4(a) and 4(b). The energy balance for splitting the As surface dimer by inserting an In atom from a remote M_1 site is slightly exothermic, in contrast to the endothermicity of 0.16 eV for the transition $M_1 \rightarrow M_D$ on the pristine InAs(137) surface.

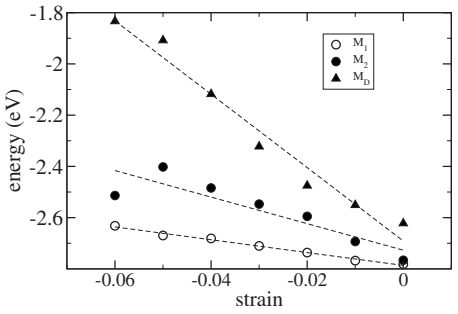

FIG. 5. Binding energy of a single In adatom occupying one of the sites M_1, M_2, or M_D, as a function of compressive isotropic surface strain. The dashed lines are guides to the eyes.

After growth has reached the stage shown in Fig. 4(b), the same structural motifs are present as on the starting surface, i.e., As surface dimers and threefold coordinated In species. Thus, one could speculate that the structure in Fig. 4(b) is an epinucleus, as defined by the nucleation theory of epitaxial growth on reconstructed surfaces,[27] while the structure in Fig. 4(a) is not yet compatible with the surface reconstruction of the new layer about to form. Formally, the structure in Fig. 4(b) has two formula units of InAs in excess of the starting surface. By considering bulk InAs as thermodynamic reservoir for these two units, we calculate that the candidate structure is still by 0.67 eV higher in energy than the bulk reservoir. Thus, whether the In-As_2-In complex can be considered as a stable epinucleus or not will depend on the growth conditions, i.e., on the nonequilibrium concentrations of surface species attainable in a particular growth experiment.

C. Effect of strain on the energetics

In order to apply the growth scenario outlined above to quantum dot growth, we need to take the compressive strain on the quantum dot side facets into account. Therefore we repeated the above calculations for the In adsorption energies, the transitions states for In diffusion, and for the stability of the growth intermediates, for a strained surface. In InAs quantum dots, InAs is coherently matched to the GaAs substrate, which has a lattice constant smaller than InAs by about 7%. Compressive strain of up to −6% was modeled in our DFT calculations by a corresponding reduction in the lateral size of the unit cell, allowing the atoms in the slab to relax along the surface normal. Those atoms that were kept fixed in the calculation were shifted along the surface normal according to the elastic response of the slab upon biaxial strain, as calculated previously.[28] The values reported in Figs. 5–8 are energy differences calculated from two slabs (e.g., a clean surface and a surface with an In adatom) at the same value of the strain.

Figure 5 shows that the adsorption energy of an In adatom is significantly reduced if the substrate surface is under com-

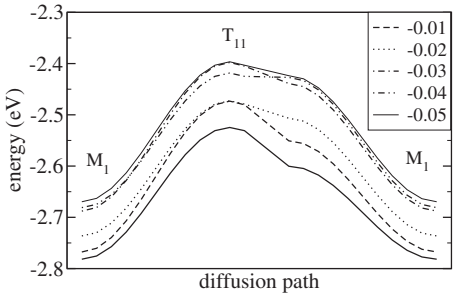

FIG. 6. Adsorption energy for an In adatom for the minima and saddle points along the "uphill" diffusion path for an isotropic surface strain between −0.05 and −0.01 (legend in the figure) and for the unstrained surface (lowest full curve).

pressive strain. This holds true for all binding sites investigated but with a different sensitivity to the amount of compressive strain. To a good approximation, our values of the adsorption energy vary linearly with the applied strain. Such a linear dependence can be understood from the difference in intrinsic surface stress between the clean surface and the surface with the In adatom.[29] We note that inserting an In adatom into the surface As dimer [site M_D, Fig. 3(c)], which is energetically unfavorable on the unstrained surface, is even more unfavorable on a biaxially compressed slab. This observation is expected as the clean InAs(137) surface is under tensile surface stress and thus lowers its energy under external compressive strain.[13] Inserting the large In atom into the As dimer reduces the tensile surface stress, rendering the surface less susceptible to external strain. Thus, the energy balance for inserting the In atom becomes even more endothermic when the surface prior to insertion was subject to compressive strain. Consequently, our previous conclusion that this adsorption site is unimportant for growth remains true for the compressively strained side facets of quantum dots.

The present calculations clearly demonstrate that the binding energy of diffusing In adatoms is significantly reduced in the highly strained region near the lower edge of a QD. During growth of the QD, In adatoms arriving from the substrate around the island need to diffuse through this region in order to attach to the top part of the QD, where growth is most favorable. Hence our present findings corroborated previous claims by us[20] and others[30,31] that a region of reduced binding energy acts like a "repulsive ring" around the quantum dot that hinders the influx of material. The strength of this repulsion increases with the size of the quantum dot. While our previous work reported repulsion due to a strained region in the substrate around the QD, the present results enhance this effect as the repulsive region now extends to (the lower part of) the QD's side facets.

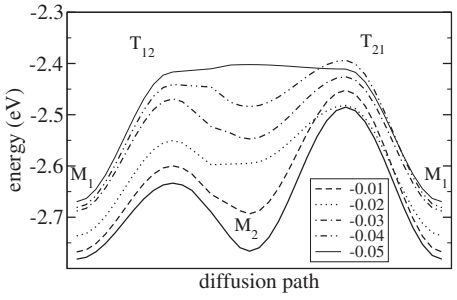

FIG. 7. Adsorption energy for an In adatom for the minima and saddle points along the "sideways" diffusion path for an isotropic surface strain between −0.05 and −0.01 (legend in the figure) and for the unstrained surface (lowest full curve).

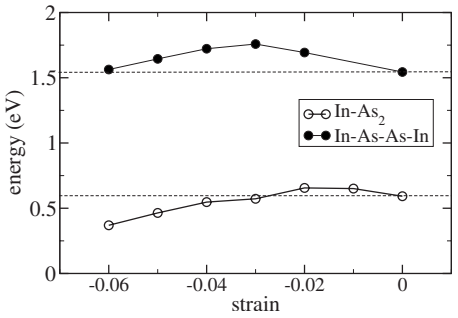

FIG. 8. Desorption energy of As_2 bound to a single In adatom [hollow symbols, cf. Fig. 4(a)] or bound to a pair of In adatoms [full symbols, cf. Fig. 4(b)] as a function of compressive isotropic surface strain. The dashed horizontal lines indicate the values of the desorption energy for the unstrained surface.

Next we discuss the effect of strain on the diffusion barriers. Our results for the "uphill" and the "sideways" diffusion pathways are shown in Figs. 6 and 7, respectively. While strain has a significant effect on the binding energies along the whole diffusion pathway, the energy changes induced at the minima and at the saddle points are roughly similar. Consequently, the activation energy for hopping, i.e., the energy difference between a saddle point and the deepest minimum M_1, is hardly sensitive to applied strain. It remains in the range of 0.25–0.3 eV even for compressive strain up to −5%. It is worth noting that the minimum M_2 becomes very shallow and eventually vanishes for a compressive strain of −0.05. We find that the potential-energy profile displays less structure if the surface is under compressive strain.

We have noted above that the likelihood of In adatoms occupying adjacent sites is strongly reduced due to repulsive adatom interactions. This tendency is found to persist under compressive strain; the repulsive interaction is even somewhat increased at the compressed substrate surface.

The effect of strain on the energy required to desorb an adsorbed As_2 molecule into the gas phase is plotted in Fig. 8. While the desorption energy of an As_2 species bound to two In adatoms [Fig. 4(b)] is large and changes only slightly with strain, the stability of the As_2 surface species attached to only one In adatom [Fig. 4(a)] is significantly reduced by compressive strain. As a result, the energy required for desorption drops below 0.4 eV for an absolute magnitude of the strain larger than 5%. Assuming about equal pre-exponential factors for In diffusion (cf. Table I) and As_2 desorption, this implies that the lifetime of the intermediate structure in Fig. 4(a) under compressive strain will be comparable to the residence time of a single In atom at any of the stable surface sites. Hence it will be unlikely under these conditions that the In-As_2 structure has the chance of capturing another In atom before the structure decays via As_2 desorption. In other words, this important intermediate stage for growth on

TABLE I. Binding energy of an In atom at the sites indicated in Fig. 2. The relaxed atomic structures resulting from the calculations are shown in Fig. 3. The double index of the transition states indicates which two minima are connected by the transition path.

M_1	M_2	M_D	T_{11}	T_{12}	T_{21}
−2.78	−2.73	−2.62	−2.52	−2.49	−2.60

InAs(137)*A* will become destabilized by the strain, and InAs growth will cease in these highly strained regions.

IV. CONCLUSIONS

Using the results of DFT calculations, we are in a position to propose a growth scenario for InAs homoepitaxy on the high-index InAs(137)*A* surface: In adatoms on this surface are highly mobile, with nearly isotropic activation energies for diffusion in the range of 0.26–0.29 eV. Growth proceeds via a short-lived intermediate state in which an As_2 species from the gas phase binds to a single In adatom. This complex is stabilized by attachment of a second In adatom. We believe that a similar growth scenario not only holds for InAs(137)*A* (which is not stable as an extended surface) but also applies to the reconstructed (113)*A* and (2 5 11)*A* surfaces of InAs, which display similar structural motifs (and are epitaxially stable). Moreover, we point out the consequences of our findings for the growth of InAs quantum dots. These self-assembled nanostructures in many cases display strained InAs(137) side facets. Our DFT calculations show that the effect of compressive strain in growth is twofold: first, In adatoms are less strongly bound in the compressively strained regions at the foothill of a quantum dot. Due to this weaker binding, the highly strained region hampers material transport from the wetting layer toward the top of the island, notwithstanding the similar diffusion barriers in strained and unstrained regions. Moreover, if QD nuclei compete for freshly deposited material diffusing on the wetting layer, the strained regions near the islands may affect the relative growth speed of the nuclei in such a way that island sizes tend to become more equal than expected from the randomly distributed nucleation events.[20] Second, and more importantly, compressive strain is found to destabilize the As_2-In growth intermediate. Without these adsorption sites for arsenic, further growth of InAs is not possible. Recently, a theoretical investigation by one of the authors[13] based on thermodynamics arguments, supported by experimental studies, suggested that small quantum dots initially grow in layer-by-layer growth on their {137} side facets. This layer growth was proposed to be incomplete due to the high strain values at the lower edges of the quantum dot. The present atomistic study provides a microscopic underpinning for the proposed evolution of InAs quantum dots.

We note possible analogies between the shape evolution of strained islands in InAs/GaAs heteroepitaxy and in other heteroepitaxial systems. Recently it has been proposed on experimental grounds that the systems Ge/Si and InAs/GaAs follow similar trends in the shape evolution of heteroepitaxially strained islands.[32] For the Ge/Si islands, incomplete facet growth is observed on the Ge(105) facet, and recent theoretical studies have revealed the atomistic mechanism of Ge diffusion[33] and layer nucleation[34] on these facets. However, the kinetic limitation of arsenic incorporation in strained regions found in the present work is a unique feature of the growth of arsenide compound semiconductors.

As a possible extension of this work, we propose to perform kinetic Monte Carlo simulations that combine calculated values of the strain on heteroepitaxial island facets with the information about the effects of strain on barrier heights obtained from the DFT calculations.

ACKNOWLEDGMENTS

We would like to thank M. Albao for help with the calculations and the European Network of Excellence SANDiE for financial support.

*peter.kratzer@uni-duisburg-essen.de

[1] K. Jacobi, L. Geelhaar, and J. Márquez, Appl. Phys. A: Mater. Sci. Process. **75**, 113 (2002).
[2] Y. Temko, T. Suzuki, and K. Jacobi, Appl. Phys. Lett. **82**, 2142 (2003).
[3] Y. Temko, T. Suzuki, P. Kratzer, and K. Jacobi, Phys. Rev. B **68**, 165310 (2003).
[4] Y. Temko, T. Suzuki, M. Xu, and K. Jacobi, Surf. Sci. **591**, 117 (2005).
[5] L. Geelhaar, J. Márquez, P. Kratzer, and K. Jacobi, Phys. Rev. Lett. **86**, 3815 (2001).
[6] L. Geelhaar, Y. Temko, J. Márquez, P. Kratzer, and K. Jacobi, Phys. Rev. B **65**, 155308 (2002).
[7] Y. Temko, L. Geelhaar, T. Suzuki, and K. Jacobi, Surf. Sci. **513**, 328 (2002).
[8] L. Geelhaar, J. Márquez, and K. Jacobi, Phys. Rev. B **60**, 15890 (1999).
[9] M. Wassermeier, J. Sudijono, M. D. Johnson, K. T. Leung, B. G. Orr, L. Däweritz, and K. Ploog, Phys. Rev. B **51**, 14721 (1995).
[10] A. Feltrin and A. Freundlich, J. Cryst. Growth **301–302**, 38 (2007).
[11] E. Placidi, A. Della Pia, and F. Arciprete, Appl. Phys. Lett. **94**, 021901 (2009).
[12] J. Márquez, L. Geelhaar, and K. Jacobi, Appl. Phys. Lett. **78**, 2309 (2001).
[13] P. Kratzer, Q. K. K. Liu, P. Acosta-Diaz, C. Manzano, G. Cos-

tantini, R. Songmuang, A. Rastelli, O. G. Schmidt, and K. Kern, Phys. Rev. B **73**, 205347 (2006).
[14] M. Bockstedte, A. Kley, J. Neugebauer, and M. Scheffler, Comput. Phys. Commun. **107**, 187 (1997).
[15] H. J. Monkhorst and J. D. Pack, Phys. Rev. B **13**, 5188 (1976).
[16] J. P. Perdew, K. Burke, and M. Ernzerhof, Phys. Rev. Lett. **77**, 3865 (1996).
[17] M. Fuchs and M. Scheffler, Comput. Phys. Commun. **119**, 67 (1999).
[18] A. Kley, P. Ruggerone, and M. Scheffler, Phys. Rev. Lett. **79**, 5278 (1997).
[19] P. Kratzer and M. Scheffler, Phys. Rev. Lett. **88**, 036102 (2002).
[20] E. Penev, P. Kratzer, and M. Scheffler, Phys. Rev. B **64**, 085401 (2001).
[21] E. Penev, S. Stojković, P. Kratzer, and M. Scheffler, Phys. Rev. B **69**, 115335 (2004).
[22] M. Rosini, P. Kratzer, and R. Magri (unpublished).
[23] K. Fujiwara, A. Ishii, and T. Aisaka, Thin Solid Films **464-465**, 35 (2004).
[24] M. Rosini, M. C. Righi, P. Kratzer, and R. Magri, Phys. Rev. B **79**, 075302 (2009).
[25] P. Kratzer, C. G. Morgan, and M. Scheffler, Prog. Surf. Sci. **59**, 135 (1998).
[26] C. T. Foxon and B. A. Joyce, Surf. Sci. **64**, 293 (1977).
[27] Raj Ganesh S. Pala and F. Liu, Phys. Rev. Lett. **95**, 136106 (2005).
[28] T. Hammerschmidt, P. Kratzer, and M. Scheffler, Phys. Rev. B **75**, 235328 (2007).
[29] L. Huang, F. Liu, and X. G. Gong, Phys. Rev. B **70**, 155320 (2004).
[30] A. Madhukar, J. Cryst. Growth **163**, 149 (1996).
[31] H. M. Koduvely and A. Zangwill, Phys. Rev. B **60**, R2204 (1999).
[32] G. Costantini, A. Rastelli, C. Manzano, R. Songmuang, O. G. Schmidt, H. von Känel, and K. Kern, Appl. Phys. Lett. **85**, 5673 (2004).
[33] F. Montalenti, D. B. Migas, F. Gamba, and L. Miglio, Phys. Rev. B **70**, 245315 (2004).
[34] S. Cereda and F. Montalenti, Phys. Rev. B **75**, 195321 (2007).